Original Article

Mitochondrial malic enzyme 2 promotes breast cancer metastasis via stabilizing HIF-1α under hypoxia

Duo You[1], Danfeng Du[2], Xueke Zhao[2], Xinmin Li[3], Minfeng Ying[1], Xun Hu[1]

[1]Cancer Institute (Key Laboratory for Cancer Intervention and Prevention, China National Ministry of Education, Zhejiang Provincial Key Laboratory of Molecular Biology in Medical Sciences), The Second Affiliated Hospital, Zhejiang University School of Medicine, Hangzhou 310000, China; [2]State Key Laboratory of Esophageal Cancer Prevention & Treatment and Henan Key Laboratory of Esophageal Cancer Research of the First Affiliated Hospital, Zhengzhou University, Zhengzhou 450000, China; [3]Department of Pathology, Women and Infants Hospital of Zhengzhou, Zhengzhou 450000, China

Correspondence to: Prof. Xun Hu, PhD. Cancer Institute (Key Laboratory for Cancer Intervention and Prevention, China National Ministry of Education, Zhejiang Provincial Key Laboratory of Molecular Biology in Medical Sciences), The Second Affiliated Hospital, School of Medicine, Zhejiang University, No. 88 Jiefang Road, Hangzhou 310000, China. Email: huxun@zju.edu.cn.

Abstract

Objective: α-ketoglutarate (α-KG) is the substrate to hydroxylate collagen and hypoxia-inducible factor-1α (HIF-1α), which are important for cancer metastasis. Previous studies have shown that the upregulation of collagen prolyl 4-hydroxylase in breast cancer cells stabilizes the expression of HIF-1α by depleting α-KG levels. We hypothesized that mitochondrial malic enzyme 2 (ME2) might also affect HIF-1α expression via modulating α-KG levels in breast cancer cells.

Methods: We evaluated ME2 protein expression in 100 breast cancer patients using immunohistochemistry and correlated with clinicopathological indicators. The effect of ME2 knockout on cancer metastasis was evaluated using an orthotopic breast cancer model. The effect of ME2 knockout or knockdown on the levels of α-KG and HIF-1α proteins in breast cancer cell lines was determined both *in vitro* and *in vivo*.

Results: ME2 was found to be upregulated in the human breast cancerous tissues compared with the matched precancerous tissues (P<0.001). The elevated expression of ME2 was associated with a poor prognosis (P=0.019). ME2 upregulation was also related to lymph node metastasis (P=0.016), pathological staging (P=0.033), and vascular cancer embolus (P=0.014). Also, ME2 knockout significantly inhibited lung metastasis *in vivo*. In the tumors formed by ME2 knockout cells, the levels of α-KG were significantly increased and collagen hydroxylation level did not change significantly but HIF-1α protein expression was significantly decreased, compared to the control samples. In cell culture, cells with ME2 knockout or knockdown demonstrated significantly higher α-KG levels but significantly lower HIF-1α protein expression than control cells under hypoxia. Exogenous malate and α-KG exerted similar effect on HIF-1α in breast cancer cells to ME2 knockout or knockdown. Additionally, treatment with malate significantly decreased 4T1 breast cancer lung metastasis. ME2 expression was associated with HIF-1α levels in human breast cancer samples (P=0.008).

Conclusions: Our results provide evidence that upregulation of ME2 is associated with a poor prognosis of breast cancer patients and propose a mechanistic understanding of a link between ME2 and breast cancer metastasis.

Keywords: Malic enzyme 2; breast cancer; metastasis; malate; α-ketoglutarate; hypoxia-inducible factor-1α

Submitted Feb 05, 2021. Accepted for publication Apr 22, 2021.
doi: 10.21147/j.issn.1000-9604.2021.03.03
View this article at: https://doi.org/10.21147/j.issn.1000-9604.2021.03.03

Introduction

Breast cancer (BC) is the most commonly diagnosed cancer and the leading cause of cancer-related death in females worldwide (1-3). There is a significant difference in the mortality rates of early, locally advanced, and metastatic cancers. According to the statistics of American Cancer Society on female BC, the 5-year survival rate for stage I, II, and III is 98%, 92%, and 75%, respectively, while for stage IV (metastatic disease) it drops to 27% (4). Metastasis accounts for 90% of BC-related fatalities (5,6). The typical features for BC include generation of regions of hypoxia and stabilization of hypoxia-inducible factor-1α (HIF-1α) protein (7,8). Previous studies have shown that HIF-1 signaling pathways play important roles in BC metastasis (7,9).

Studies have demonstrated that regulation of α-ketoglutarate (α-KG) levels affects the stability of HIF-1α protein in BC cells. Also, collagen prolyl-4-hydroxylase (P4H) expression has been correlated with α-KG levels in BC cells (10-12). P4H is known to be upregulated in BC cells (11,12). The upregulated expression of P4H uses α-KG to hydroxylate the collagen, thereby reducing the concentration of cellular α-KG, which, in turn, decreases the activity of HIF-1-prolyl hydroxylase (HIF-PHDs) and stabilizes the expression of HIF-1α protein, enhancing cancer cell metastasis (10-12).

α-KG is mainly produced in the flux of tricarboxylic acid cycle (TCAC). We hypothesized that mitochondrial malic enzymes (MEs) could potentially regulate α-KG levels in BC cells. MEs catalyze the oxidative decarboxylation of malate, and hence the upregulated expression of MEs could deplete malate levels in the flux of TCAC and potentially decrease the concentration of TCAC intermediates, including α-KG. Mitochondrial MEs include two isoforms, the NAD(P)$^+$-dependent ME2, and the NADP$^+$-dependent ME3 (13-15). As the major isoform in mitochondria of the MEs family (16), knockdown of ME2 by shRNA has been shown to promote an accumulation of TCAC intermediates in lung cancer cells (17). As ME2 could regulate HIF-1α stability via modulating the concentration of α-KG, we propose that ME2 expression is directly associated with BC metastasis. Until now, there is a lack of studies on the relationships between ME2 expression and α-KG, between ME2 expression and HIF-1α stability, and between ME2 expression and BC metastasis.

ME2 is known to play various roles in cancer. There is an inverse relationship between the expression of p53 and ME2, i.e., the downregulation of ME2 expression activates p53, inducing senescence (16). ME2 expression is found to be correlated to disease progression of melanoma (18) and glioma (19). Additionally, ME2 knockdown leads to AKT inhibition (17) and AMPK activation (16). Pharmacological inhibition of ME2 has been shown to induce cellular senescence (20), and silencing of ME2 sensitizes the head and neck squamous cell carcinoma cells to therapy-induced senescence (21). However, the relationship between ME2 and BC metastasis is still unclear.

Here, we aim to investigate if ME2 knockout or knockdown could decrease HIF-1α protein expression by increasing the concentration of α-KG in BC cells, inhibiting BC cell metastasis, to provide a mechanistic understanding of a link between ME2 and BC metastasis.

Materials and methods

Cells

BC cell lines 4T1 and MDA-MB-231 were purchased from Cell Bank of Type Culture Collection of the Chinese Academy of Science (Shanghai, China). Cell lines were identified using DNA fingerprinting (SNP for 4T1 and STR for MDA-MB-231) and confirmed to be mycoplasma free. 4T1 was cultured in RPMI-1640 supplemented with 10% foetal bovine serum (FBS) and 1% penicillin/streptomycin and 2 mmol/L L-glutamine. MDA-MB-231 was cultured in L15 medium supplemented with 10% FBS and 1% penicillin/streptomycin and 2 mmol/L L-glutamine. A flow cell counter (JIMBIO) was used for cell counting and cell size measurement.

Reagents, enzymes and antibodies

Reagents including the following: ADP (Sigma, A5285, St. Louis, USA), NAD (Sigma, N0632), NADH (Sigma, N8129), malate acid (Sigma, 02288), α-ketoglutaric acid (Sigma, 75890), dimethyl malate (Sigma, 374318), and dimethyl 2-oxoglutarate (Sigma, 349631). Enzymes including the following: malic dehydrogenase (Sigma, M2634), L-glutamic dehydrogenase (Sigma, G2501), and citrate synthase (Roche, 2168342). Antibodies including the following: ME2 (Abcam, 139686, Cambridge, USA), HIF-1α (Abcam, 16066), and β-actin (HUABIO, M1210-2, Hangzhou, China).

ME2 knockout in 4T1 cells

The ME2 knockout was done using CRISPR-Cas9 system

in 4T1 cells following a standard protocol (22). The designed sgRNA sequences were as follows: ME2 forward: CACCGTTACAAGAGCGACAAATGCT, ME2 reverse: AAACAGCATTTGTCGCTCTTGTAAC.

A pSpCas9 (BB)-2A-Puro (PX459) v2.0 plasmid (Addgene; #62988) was used as the sgRNA expression vector and Lipofectamine 3000 (Invitrogen, Carlsbad, USA) was used to transfect the constructed plasmids into the cells. Puromycin and T7 endonuclease I were used to select the cells and assess the cleavage efficiency. The monoclonal cell lines were cultured and microdeletion was detected using polymerase chain reaction (PCR) and Sanger sequencing. The candidate off-target sites were checked via sequencing to avoid the off-target effect. The ME2 knockout sequences was identified by gene sequencing (*Supplementary Figure S1A*), and the effect of ME2 knockout was analyzed by western blot using anti-ME2 antibodies (*Supplementary Figure S1B*).

ME2 knockdown in MDA-MB-231 cells

For ME2 knockdown in MDA-MB-231 cells, three specific short hairpin RNA (shRNA) were chemically synthesized by Sangon Biotech (Shanghai, China). The three ME2 shRNA sequences used in this study were as follows: ishME2#1: (CCGGCGGCATATTAGTGACAGTGTTC TGCAGAACACTGTCACTAATATGCCGTTTTTG), ishME2#2: (CCGGCCCAGTATGGACACATCTTTAC TGCAGTAAAGATGTGTCCATACTGGGTTTTTG), ishME2#3: (CCGGGCACGGCTGAAGAAGCATATAC TGCAGTATATGCTTCTTCAGCCGTGCTTTT TG).

The expression plasmids for ME2 shRNA were made in pLKO.1-puro vector (Addgene, #10879, Cambridge, USA) using the protocol provided by Addgene. The shME2-expressing pLKO.1 vector was introduced into cancer cell lines by lentiviral infection. The recombinant lentiviral particles were produced by transient transfection of HEK293T cells following a standard protocol. Briefly, cells were maintained in standard culture conditions without any antibiotics. The recombinant pLKO.1-shME2 plasmid was transfected into HEK293T cells using the packaging vectors. The viral supernatant was harvested 72 h post-transfection, centrifuged to remove any HEK293T cells, and purified by ultracentrifugation. The packaged pLKO.1-shME2 lentiviral particles were added to cell culture medium containing polybrene (4 μg/mL). After infection for 72 h, cells were selected using puromycin (1.5 μg/mL) and the effect of knockdown was analyzed by western blot using anti-ME2 antibodies (*Supplementary Figure S1C*). A non-targeting shRNA (shPLKO) was used as a control.

Hypoxia treatment of cells

Cells were seeded into 10 cm dishes and incubated overnight in a normoxic incubator. Once the density of cells reached 70%−80%, the medium was replaced with standard medium (supplemented with 10% FBS and 2 mmol/L L-glutamine without any antibiotic). For exogenous α-KG treatment, the medium was replaced with standard medium supplemented with 0.5 mmol/L or 1 mmol/L dimethyl α-KG. For exogenous malate treatment, the medium was replaced with standard medium supplemented with 10 mmol/L or 20 mmol/L dimethyl malate. Then, cells were transferred into a hypoxic culture chamber (ELECTROTEK, England) and incubated for 4 h with 1% O_2 and 5% CO_2.

Western blot

Cells and tumor tissues were lysed with M-PERTM mammalian protein extraction reagent (Thermo Fisher Scientific, Waltham, USA). Protein concentration was determined using the BCA protein assay kit (Thermo Fisher Scientific). Briefly, 1.5×10^6 4T1 or 8×10^5 MDA-MB-231 cells were seeded in a 6-well plate, after hypoxic treatment, rinsed twice with ice-cold PBS, followed by the addition of 80 μL ice-cold M-PERTM, containing protease inhibitor (Master of Small Molecules, New Jersey, USA). Then, the plates were scraped and the suspension was removed into an Eppendorf tube. All the above operations were carried out in the hypoxic incubator with 1% O_2. The cell suspension was centrifuged (10,000 r/min, 4 °C, 5 min). The supernatant was collected and mixed with loading buffer, containing 100 mmol/L dithiothreitol (DTT), and boiled for 10 min. Next, the protein extract (40 μL) was separated by 10% SDS-PAGE, transferred to PVDF membranes, and blocked with 5% bovine serum albumin for 1 h. Then the membranes were incubated overnight with primary antibodies (β-actin 1:5,000; ME2 1:2,000; HIF-1α 1:1,000) at 4 °C. The HRP-conjugated secondary antibodies (1:5,000) were added and protein bands were visualized by enhanced chemiluminescence (Tanon, China).

For protein extraction from tumor tissues, 50 mg tumor tissue was minced, mixed with 1.5 mL of ice-cold M-

PERTM, containing protease inhibitor and then homogenized. The homogenized tissue was centrifuged (10,000 r/min, 4 °C, 10 min). The supernatant was collected and sample (40 μL) was mixed with loading buffer for western blot as previously described.

Enzymatic determination of malate, α-KG, and citrate

After hypoxia treatment, cells were harvested as follows: the cells were rinsed thrice with ice-cold PBS, followed by the addition of 1.2 mL of 80% (v/v) methanol per well. Next, the plates were scraped and the suspension was removed into an Eppendorf tube. The above-mentioned protocol was performed in a hypoxic incubator with 1% O_2. Next, the lysate/methanol mixture was mixed well and centrifuged (14,000 r/min, 10 min, 4 °C) to remove the debris. The supernatant was completely evaporated, and the lyophilized sample was dissolved in 400 μL double distilled water, followed by centrifugation (14,000 r/min, 10 min, 4 °C). The supernatant was collected for subsequent metabolite analysis. For tumor tissue, tumor tissue (200 mg) was minced, 1.0 mL of 80% (v/v) methanol was added, and then homogenized on ice. The mixture was mixed well and centrifuged at 14,000 r/min for 10 min at 4 °C. The supernatant was evaporated, and the lyophilized sample was dissolved in 400 μL of double distilled water, centrifuged, and the supernatant was collected as previously described. The concentrations of metabolite were measured using a spectrophotometer (Beckman Coulter, Brea, USA) following a previously described method with minor modifications (23).

Assay for malate

We added 20 μL of the sample to 980 μL of the reaction buffer (200 mmol/L Glycine, 170 mmol/L hydrazine, 2 mmol/L NAD^+, 2.1 U/mL malic dehydrogenase, pH=9.2). The sample was mixed well and incubated at room temperature for 1 h, and the absorbance was recorded at 340 nm against the blank (20 μL sample without the enzyme).

Assay for α-KG

We added 100 μL of the sample to 900 μL of the reaction buffer (40 mmol/L imidazole, 20 mmol/L acetate, 25 mmol/L ammonium acetate, 100 μmol/L ADP, 100 μmol/L NADH, 0.15 U/mL L-glutamic dehydrogenase). The sample was mixed well and incubated at room temperature for 15 min, and the absorbance was recorded at 340 nm against the blank (100 μL sample without the enzyme).

Assay for citrate

We added 50 μL of the sample to 950 μL of the reaction buffer (25 mmol/L Tris-base, 75 mmol/L Tris-HCl, 100 μmol/L NADH, 40 μmol/L $ZnCL_2$, 0.12 U/mL citrate lyase, 0.3 U/mL malic dehydrogenase, pH=7.6). The sample was mixed well and incubated at room temperature for 10 min, and the absorbance was recorded at 340 nm against the blank (50 μL sample without the enzyme).

Transfection of 4T1 cell with luciferase gene

A pcDNA3.1(+) (Invitrogen, #V790-20) plasmid was used as the expression vector. The coding sequence of the luciferase gene was cloned and ligated with the expression vector. The resultant recombinant-retrovirus contained the expressing luciferase gene. The recombinant lentiviral particles were produced by transient transfection of HEK293T cells following a standard protocol as previously described. For lentiviral infection, $4T1_{PX459}$ or $4T1_{ME2KO}$ cells were seeded in a 6-well plate and the retrovirus was added to the cell culture medium containing polybrene (4 μg/mL). After infection for 72 h, cells were selected using G418. The surviving cells were designated as $4T1_{PX459\text{-}Luciferase}$ or $4T1_{ME2KO\text{-}Luciferase}$. The *in vitro* luciferase activity of the cells was determined using a standard approach. We collected 8×10^5 cells and lysed in 1× passive lysis buffer. We mixed cell lysate (98 μL), 2 μL of luciferin stock solution (15 mg/mL) and 100 μL of luciferase assay buffer (200 mmol/L Tris- HCl pH 7.8, 10 mmol/L $MgCl_2$, 500 μmol/L CoA, 300 μmol/L ATP) and recorded the absorbance at 560 nm.

Orthotopic tumor growth and metastasis assays in mouse model

Six-week-old female BALB/c mice were randomly assigned to two groups (n=6 per group) and orthotopically inoculated with 1×10^5 $4T1_{PX459}$ or $4T1_{ME2KO}$ cells near the second right mammary fat pad. The mouse weight and tumor size were measured weekly. The mouse tumor volume (V) was calculated using the following formula: V (cm^3) = [length (cm) × width (cm) ^{2} × 0.5]. The mice were sacrificed after 5 weeks, tumor weight was recorded, and the lung metastasis was scored by counting the macroscopic metastatic nodules. The $4T1_{PX459\text{-}Luciferase}$ or $4T1_{ME2KO\text{-}Luciferase}$ cells were orthotopically inoculated as previously

described to present the lung metastasis intuitively. Live animal bioluminescence imaging was used to image the tumor and lung every week after implantation (Caliper IVIS system, PerkinElmer). Isoflurane-anesthetized mice were intraperitoneally injected with D-luciferin substrates (YEASEN; 15 mg/mL in PBS) and were imaged after 10 min. All animal experiments complied with the ARRIVE guidelines and the National Institutes of Health guide for the care and use of laboratory animals and were approved by the Committee of Animal Experimental Centre at the Zhejiang Chinese Medical University.

Malate treatment in mouse model

We implanted 1×10^5 4T1 cells orthotopically into the mammary fat pads of BALB/c mice (n=12). The mice were randomly divided into two groups (n=6/per group). The malate treatment group was injected intraperitoneally with malate (50 mg/kg, dissolved in PBS) daily for three weeks. The control group was intraperitoneally injected with equal volume of PBS as control.

Hydroxyproline detection in mouse tumor tissue

Hydroxyproline is found almost exclusively in the protein collagen and is used as a marker to quantify the level of tissue collagen. The content of hydroxyproline was measured using the Hydroxyproline Assay Kit (Nanjing Jiancheng Bioengineering Institute, Nanjing, China) following the manufacturer's protocol.

Patients

All patients had undergone mastectomy between August 2012 and December 2014. The inclusion criteria were as follows: 1) patients were pathologically diagnosed with BC and had undergone surgical treatment; 2) patients had not received any radiotherapy, chemotherapy, or targeted therapy before operation; 3) complete clinicopathological records were available; and 4) patients who had other malignant tumors were excluded. The pathological staging for BC was based on American Joint Committee on Cancer (AJCC) TNM staging system in 2017 (24). All patients were females with a mean age of 48.39±11.13 years, with a median age of 46 (range, 26–82) years. The last follow-up was May 2020. The overall survival (OS) time was calculated from the day of mastectomy to death or to the last follow-up date. The median follow-up of the entire cohort was 73.5 (range, 11.7–94.0) months. Informed consent was obtained from all patients in this study. The study protocol complied with the Code of Ethics of the World Medical Association (Declaration of Helsinki) for experiments involving humans and approved by the Medical Ethics Committee of Zhengzhou University.

Immunohistochemical (IHC) analysis

We collected 100 BC tissues and 96 adjacent non-cancerous tissues from surgically resected specimens. Histopathological diagnoses were based on World Health Organization (WHO) criteria (2012) (25). The tissues were fixed in 10% neutral formalin, embedded in paraffin, and then sectioned. Serial 4-μm sections were used for histopathological analysis using hematoxylin and eosin staining. Following the manufacturer's instructions, tissue sections were deparaffinized, rehydrated, and subjected to antigen retrieval. The samples were incubated overnight with primary antibody (ME2: 1:75, HIF-1α: 1:200) at 4 °C, followed by incubation with horseradish peroxidase-conjugated secondary antibody. The immunoreactivity was visualized by adding diaminobenzidine and subsequently counterstained with hematoxylin. The sections were analyzed under microscope by two pathologists independently who were blinded to the patients' clinical information.

According to IHC scoring system described previously (26,27), ME2 immunostaining score (S) was determined semi-quantitatively by multiplying the percentage of positive cells (P) with intensity (I), using the following formula: S=P×I. The range score for percentage of positive cells was 0–4 (0, 0–10%; 1, 11%–25%; 2, 26%–50%; 3, 51%–75%; 4, 76%–100%). The range score for intensity was 0–3 (0, no staining; 1, weak; 2, moderate; 3, strong). The index score was obtained in a range from 0 to 12. The final immunostaining results were denoted as low expression of ME2 (≤6 scores) and high expression of ME2 (>6 scores). Since active HIF-1α is commonly assumed to be located in the nucleus and nuclear staining was evaluated as positive expression (28,29). Cytoplasmic staining was observed in some cases but was not recorded in this study. The positive staining for HIF-1α was defined as nuclear staining in ≥10% of the tumor cells.

Statistical analysis

Statistical analyses were conducted using IBM SPSS Statistics (Version 21.0; IBM Corp., New York, USA). Quantitative data were represented as the $\bar{x}\pm s$ and analyzed by the Student's *t*-test. Categorical data were represented as

frequency (number-percent). The difference of ME2 expression in cancerous and precancerous tissues was analyzed using McNemar's test. The relationship between ME2 expression and clinicopathological features was evaluated by the χ^2-test. The Kaplan-Meier survival analysis was used to estimate the association between eligible variables and survival. Cox proportional hazards regression model was used for multivariate survival analysis in a stepwise regression manner. A P<0.05 was considered as statistically significant.

Results

ME2 was associated with a poor prognosis in BC patients

We hypothesized that if ME2 was associated with BC metastasis, then ME2 expression of BC would be inversely correlated with the survival of BC patients.

We retrieved medical history of 100 BC patients. *Table 1* summarizes the clinicopathological characteristics of the patients. All the patients had confirmed diagnosis of BC and were predominately at the invasive stage (92.0%), only 8.0% were at the Tis stage. Of all the patients in this study, more than half of the patients were in T2 (63.0%), followed by T1 (26.0%), Tis (8.0%), and T3 (3.0%). Also, approximately half of the patients (42.0%) had positive lymph node metastasis when they were diagnosed. And 72.0% of the patients were in the earlier stage based on pathological staging, including 8.0% of patients in stage 0, 20.0% in stage I, 44.0% in stage II, and the remaining (28.0%) patients were in advanced stage III (*Table 1*).

The IHC staining analyses were performed on the specimens from 100 patients with BC, which showed that the immunoreactivity for ME2 protein was located in the cytoplasm both in cancerous and precancerous tissues (*Figure 1A*). Elevated expression of ME2 was found in breast cancerous tissues (63.0%, 63/100) compared to the matching precancerous tissues (33.3%, 32/96) (P<0.001, *Figure 1B*).

BC patients who had elevated expression of ME2 had a lower survival rate than patients with low expression of ME2 (χ^2=5.527, P=0.019, *Figure 1C*).

ME2 was associated with metastasis-related indicators

We analyzed the association between ME2 expression and clinicopathological indicators. Elevated ME2 expression was associated with lymph node metastasis (χ^2=5.405, P=0.016), pathological staging (χ^2=4.118, P=0.033), and vascular cancer embolus (χ^2=5.596, P=0.014), which were the clinicopathological indicators that are significantly correlated with metastasis and progression in BC (*Table 2*).

Table 1 Clinicopathological characteristics of 100 breast cancer patients

Variables	n (%)
Age (year)	
<50	60 (60.0)
≥50	40 (40.0)
Gender	
Male	0 (0)
Female	100 (100)
T staging	
Tis	8 (8.0)
T1	26 (26.0)
T2	63 (63.0)
T3	3 (3.0)
Lymph node metastasis	
Yes	42 (42.0)
No	58 (58.0)
Pathological staging	
0	8 (8.0)
I	20 (20.0)
II	44 (44.0)
III	28 (28.0)

Furthermore, in this study, lymph node metastasis showed a strong association with poor prognosis (χ^2=10.989, P=0.001, *Figure 2A*). Patients with positive vascular cancer embolus seemed to have a poor survival rate, but the difference was not statistically significant (χ^2=1.268, P=0.260, *Figure 2D*). In the subgroup analysis, elevated expression of ME2 exhibited a significantly worse prognostic impact on the subgroup of patients with no lymph node metastasis (χ^2=4.664, P=0.031, *Figure 2B*), or without vascular cancer embolus (χ^2=6.473, P=0.011, *Figure 2E*). However, in the subgroup of patients with lymph node metastasis (χ^2=0.374, P=0.541, *Figure 2C*), or with positive vascular cancer embolus (χ^2=0.184, P=0.668, *Figure 2F*), ME2 expression showed no significant difference in the survival rate.

Additionally, there was no significant association between ME2 expression and age group, or T staging, estrogen receptor (ER) status, progesterone receptor (PR) status, human epidermal growth factor receptor 2 (HER-2) status, and Ki67 index (*Table 2*). Pathological staging was divided into earlier staging (0–IIA) and advanced staging

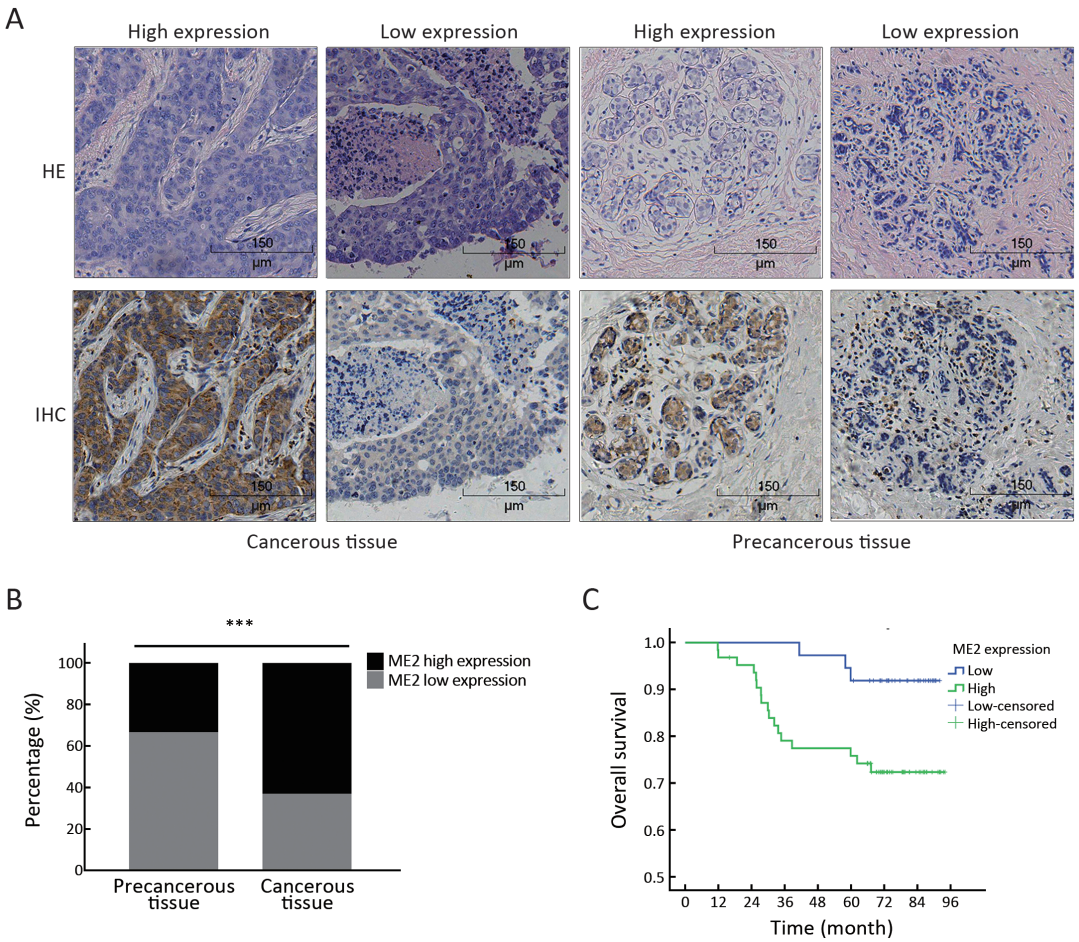

Figure 1 Expression of ME2 in breast cancer and precancerous tissues and its association with OS. (A) Representative HE and IHC staining of ME2 in human breast cancerous and precancerous specimens. The scale bar is 150 μm; (B) The elevated expression of ME2 was displayed in cancerous tissues compared to the matched precancerous tissues; (C) Patients with elevated expression of ME2 in breast cancerous tissue had a worse OS than those with low expression (P=0.019). Survival analyzed by Kaplan-Meier method. ***, P<0.001. ME2, malic enzyme 2; OS, overall survival; HE, hematoxylin and eosin; IHC, immunohistochemistry.

(IIB–III). The advanced staging was a poorer indicator of survival compared to the earlier staging (χ^2=12.711, P<0.001, *Supplementary Table S1*). We found no statistical difference between survival and age group, T staging, and vascular cancer embolus, respectively (*Supplementary Table S1*). The multivariate cox regression analysis demonstrated that lymph node metastasis but not ME2 was an independent prognostic risk factor for BC patients' survival (HR=3.878, P=0.010, *Supplementary Table S1*).

ME2 knockout significantly inhibited lung metastasis

These results demonstrated that ME2 expression was closely associated with BC patients' survival and metastasis-related indicators. Next, we tried to validate the relationship between ME2 and BC metastasis. We performed ME2 knockout in 4T1 cells ($4T1_{ME2KO}$) and inoculated $4T1_{ME2KO}$ and control cell $4T1_{PX459}$ into the mammary pad of BALB/c mice. Both groups of mice showed similar body weights and tumor growth (*Figure 3A–C*). However, knockout of ME2 nearly abolished 4T1 lung metastasis (*Figure 3D–F*). These results provided evidence that ME2 promoted BC metastasis.

ME2 knockout increased α-KG concentration and decreased HIF-1α protein level in BC cells in vivo

Next, we determined if ME2 knockout increased the concentration of α-KG and decreased HIF-1α levels in tumors. We found increased levels of α-KG, together with

Table 2 Relationship between ME2 expression and clinicopathological indicators in breast cancer

Variables	No. of patients examined	Expression of ME2 protein [n (%)]		χ^2	P
		High (N=63)	Low (N=37)		
Age (year)				1.401	0.166
<50	60	35 (58.3)	25 (41.7)		
≥50	40	28 (70.0)	12 (30.0)		
T staging				1.120	0.200
Tis+T1	34	19 (55.9)	15 (44.1)		
T2+T3	66	44 (66.7)	22 (33.3)		
Lymph node metastasis				5.405	0.016
No	58	31 (53.4)	27 (46.6)		
Yes	42	32 (76.2)	10 (23.8)		
Pathological staging				4.118	0.033
0+I+IIA	60	33 (55.0)	27 (45.0)		
IIB+III	40	30 (75.0)	10 (25.0)		
Vascular cancer embolus				5.596	0.014
No	83	48 (57.8)	35 (42.2)		
Yes	17	15 (88.2)	2 (11.8)		
ER status				0.018	0.530
Negative	37	23 (62.2)	14 (37.8)		
Positive	63	40 (63.5)	23 (36.5)		
PR status				2.581	0.081
Negative	40	29 (72.5)	11 (27.5)		
Positive	60	34 (56.7)	26 (43.3)		
HER-2 status				0.429	0.807
Negative	42	25 (59.5)	17 (40.5)		
Positive	36	24 (66.7)	12 (33.3)		
Not available	22	14 (63.6)	8 (36.4)		
Ki67 index (%)				0.249	0.395
≤14	24	14 (58.3)	10 (41.7)		
>14	75	48 (64.0)	27 (36.0)		

ME2, malic enzyme 2; ER, estrogen receptor; PR, progesterone receptor; HER-2, human epidermal growth factor receptor 2.

malate and citrate, in $4T1_{ME2KO}$-derived tumor compared with control tumors (P<0.05, *Figure 4A–C*). As the substrate of 2-oxoglutarate dependent oxygenases, α-KG is known to be involved in collagen stabilization and HIF-1α degradation, both of which are correlated to tumor metastasis (30,31). Next, we determined the concentration of collagen hydroxyproline and HIF-1α in tumors formed by ME2 knockout 4T1 and control cells. While the levels of collagen hydroxyproline were comparable between the two groups (*Figure 4D*), HIF-1α protein expression was significantly lower in ME2 knockout group than in the control group (P<0.01, *Figure 4E–G*).

ME2 knockout or knockdown increased α-KG concentration and decreased HIF-1α level in BC cells under hypoxia

These results suggested that ME2 knockout increased α-KG levels and decreased HIF-1α protein expression but it did not necessarily indicate that the increased α-KG and decreased HIF-1α levels were directly linked to ME2, because cancer cells *in vivo* are known to be present in a complex and dynamic environment. Next, we measured the α-KG levels and HIF-1α protein expression in ME2 knockout cells $4T1_{ME2KO}$ and ME2 knockdown cells MDA-MB-231_{shME2} cultured under hypoxia to further link

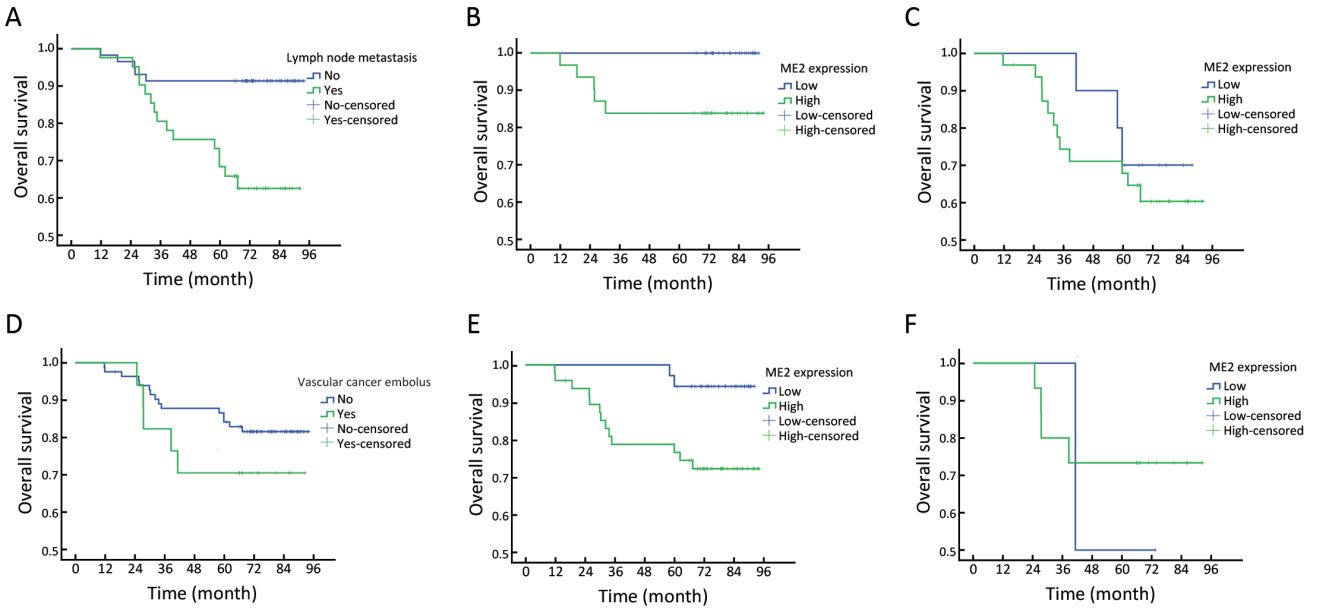

Figure 2 ME2 is associated with metastasis-related indicators. (A) Lymph node metastasis status showed a clear association with poor prognosis (χ^2=10.989, P=0.001); (B) In subgroup of patients with no lymph node metastasis, elevated ME2 expression was a worse indicator for prognosis (χ^2=4.664, P=0.031); (C) In subgroup of patients with lymph node metastasis, ME2 expression had no significant effect on OS (χ^2=0.374, P=0.541); (D) There was no significant survival difference in patients with or without vascular cancer embolus (χ^2=1.268, P=0.260); (E) In subgroup of patients without vascular cancer embolus, elevated ME2 expression was associated with poor prognosis (χ^2=6.473, P=0.011); (F) In subgroup of patients with vascular cancer embolus, ME2 expression had no significant effect on OS (χ^2=0.184, P=0.668). Survival was analyzed by the Kaplan-Meier method. ME2, malic enzyme 2; OS, overall survival.

the relationship between ME2, α-KG, and HIF-1α. In ME2 knockout model, the effect of ME2 on α-KG concentration and HIF-1α stability could be maximized. However, the complete silence represents an extreme condition, which may cause artifact. To confirm the relationship of ME2 with α-KG and HIF-1α, we also used shRNA knockdown to partially silence ME2. If the relationship exists, then the effect of ME2 knockout or knockdown should yield similar results.

HIF-1α protein expression in the ME2 knockout or knockdown cell was significantly lower than that in control cells (*Figure 5A*,*B*), while cellular α-KG concentration was significantly higher in the ME2 knockout or knockdown cells (*Figure 5C*,*D*). Besides α-KG, malate and citrate concentrations were also elevated in the ME2 knockout or knockdown cells (*Figure 5C*,*D*).

Next, we added dimethyl α-KG into the cell culture to link α-KG with HIF-1α under hypoxia. Dimethyl α-KG is a cell membrane permeable ester; once it crosses the cell membrane, it is hydrolyzed by esterase to generate α-KG. We observed that dimethyl α-KG significantly reduced HIF-1α concentrations in 4T1 or MDA-MB-231 cells (*Figure 5E*,*F*).

The direct consequence of ME2 knockout or knockdown was the accumulation of malate, hence adding exogenous malate might mimic the effects of ME2 inhibition. The addition of exogenous dimethyl malate significantly increased the concentrations of α-KG, malate, and citrate (P<0.05, *Figure 6A*,*B*) and reduced HIF-1α protein levels in 4T1 or MDA-MB-231 cells under hypoxia (*Figure 6C*,*D*).

Malate treatment significantly inhibited lung metastasis of 4T1 BC cells

Since ME2 knockout significantly suppresses 4T1 lung metastasis, we ask if malate treatment could also inhibit BC metastasis. 4T1 cells were implanted orthotopically into mammary fat pads of BALB/c mice. Mice were randomly divided into two groups and injected intraperitoneally with phosphate buffer saline (control) or malate (50 mg/kg, dissolved in PBS) once a day for three weeks. While there was no significant difference in the mouse body weight and tumor volume between two groups (*Figure 6E*,*F*), and the metastatic nodules in lung in the malate treatment group significantly reduced (*Figure 6G*,*H*).

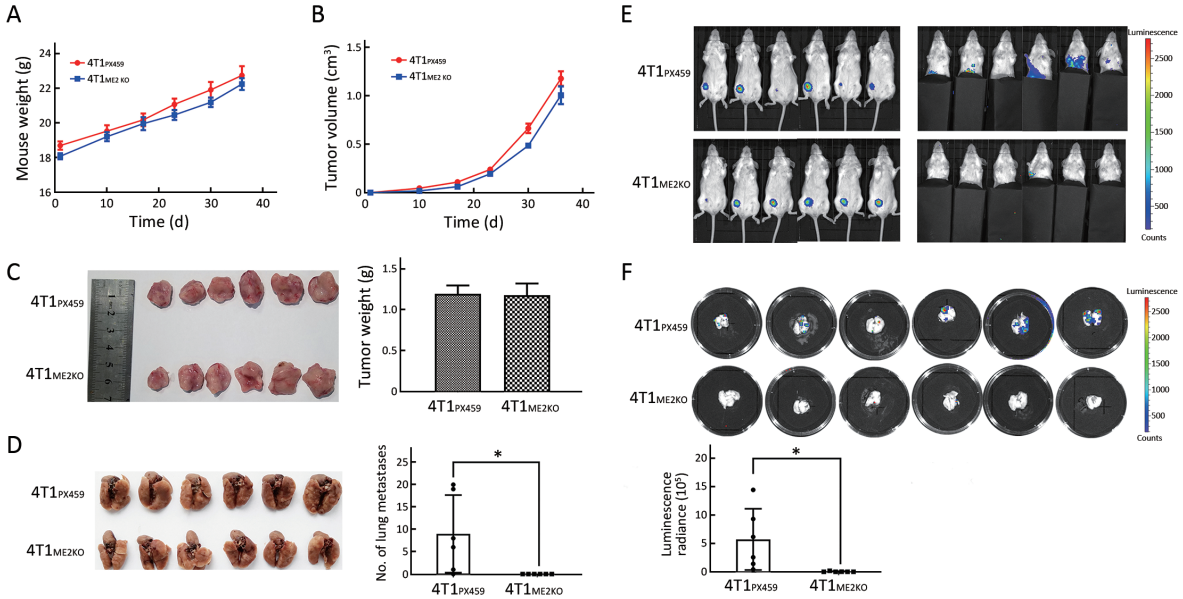

Figure 3 ME2 knockout significantly inhibits breast cancer lung metastasis *in vivo*. Six-week-old female BALB/c mice were orthotopically inoculated with 1×10^5 4T1 cells, sacrificed after 5 weeks. The tumor weight was recorded, and lung metastasis was scored. (A,B) Body weight and tumor growth curve of BALB/c mice inoculated with $4T1_{ME2KO}$ and control $4T1_{PX459}$; (C) Tumor size and weight; (D) Lung metastatic nodules; (E) Bioluminescence intensity of tumors formed by $4T1_{ME2KO}$ and control $4T1_{PX459}$. (Left panels) primary tumor. The strong bioluminescence intensity of primary tumors shadowed the bioluminescence of the lung metastasis. (Right panels) Bioluminescence emitted by lung metastasis was revealed after primary tumor bioluminescence was covered up; (F) Bioluminescence imaging of the lungs from mice inoculated with $4T1_{ME2KO}$ or $4T1_{PX459}$. n=6 per group. *, P<0.05. Data of (A–D) and (E,F) are from two independent experiments. ME2, malic enzyme 2.

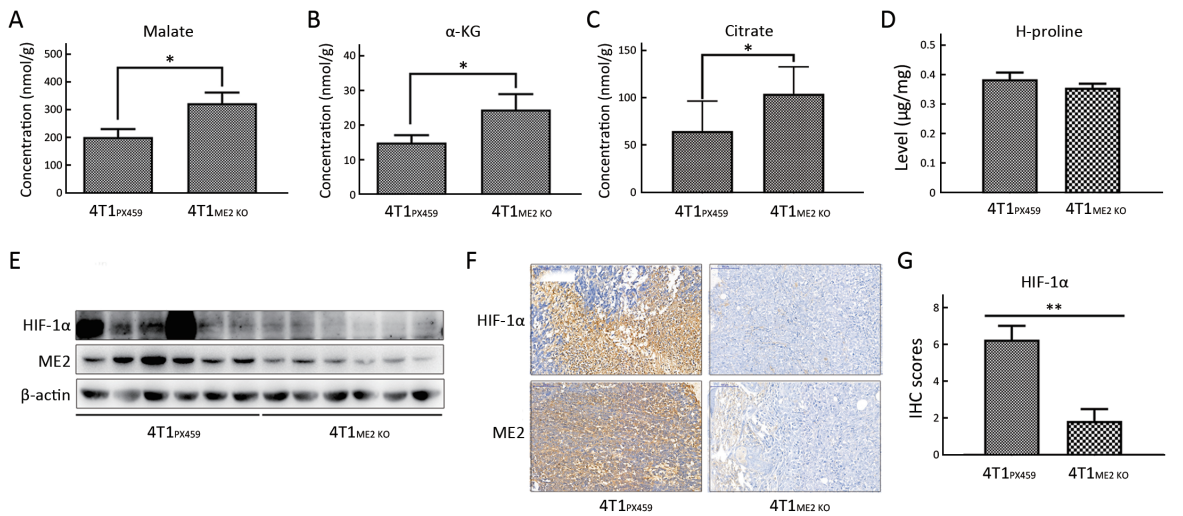

Figure 4 ME2 knockout reduces HIF-1α level and increases the concentrations of TCAC intermediates *in vivo*. The metabolite of mouse tumor tissue was extracted for analysis. (A–C) $4T1_{ME2KO}$-derived tumor tissues had a higher concentration (nmol/g wet tissues) of malate, α-KG, and citrate than $4T1_{px459}$-derived tumors; (D) Level of collagen hydroxyproline (H-proline) was comparable between the two groups; (E–G) Western blot and IHC of HIF-1α expression in $4T1_{ME2KO}$-derived and $4T1_{PX459}$-derived tumors. The expression of ME2 in $4T1_{ME2KO}$-derived tumors was probably due to the interstitial cells. n=6 per group. *, P<0.05; **, P<0.01. ME2, malic enzyme 2; HIF-1α, hypoxia-inducible factor-1α; TCAC, tricarboxylic acid cycle; α-KG, α-ketoglutarate; IHC, immunohistochemistry.

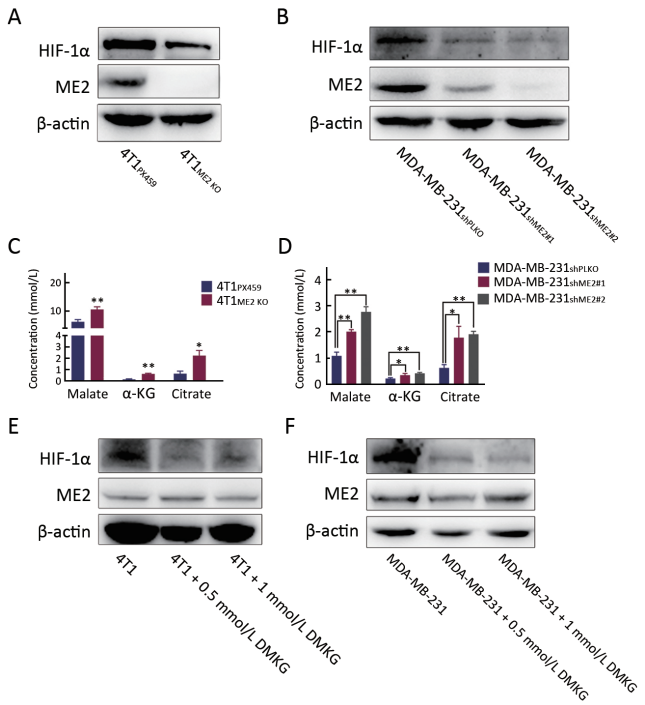

Figure 5 ME2 knockout or knockdown increases concentrations of TCAC intermediates and decreases HIF-1α level. Cells (4T1 and MDA-MB-231) were cultured under 1% oxygen for 4 h and then analyzed. (A,B) HIF-1α levels in ME2 knockout or knockdown cells and control cells; (C,D) Concentrations of TCAC intermediates malate, citrate, and α-KG in ME2 knockout or knockdown cells and control cells; (E,F) HIF-1α in 4T1 and MDA-MB-231 with or without dimethyl α-KG (DMKG) under hypoxia. *, P<0.05; **, P<0.01. ME2, malic enzyme 2; TCAC, tricarboxylic acid cycle; HIF-1α, hypoxia-inducible factor-1α.

ME2 was associated with HIF-1α expression in human BC

Next, we examined the expression of HIF-1α and ME2 in BC tissues to correlate ME2 with HIF-1α in clinical BC. The immunoreactivities of HIF-1α were located mostly in the nuclei and the cytoplasmic staining was observed in only a few cases (*Figure 7A*). Of the 100 BC patients, the positive HIF-1α expression rates were 29.7% in patients with low ME2 expression and 57.1% in patients with high ME2 expression (χ^2=7.032, P=0.008, *Figure 7B*). Elevated ME2 expression was significantly correlated to HIF-1α positive expression in human BC.

Discussion

BC metastasis is closely associated to hypoxia (8,32). The partial pressure of O_2 in BC has a median value of 10 mmHg compared to 65 mmHg in normal human breast tissue (33,34). Hypoxia enhances HIF-1 signaling, which increases the risk of metastasis (9,35,36). HIF-1 is known to target genes involved in cell survival, angiogenesis, metabolism, immortalization, metastasis, and resistance to therapy (37-39). Therefore, stabilization of HIF-1 is crucial for BC progression. HIF-1 is composed of two subunits: HIF-1α and HIF-1β. HIF-1β is constitutively expressed and is stable whereas HIF-1α is sensitive to oxygen levels. In the presence of oxygen, α-KG, and Fe^{2+}, HIF-PHDs hydroxylate HIF-1α and label it for proteasome degradation. The activity of HIF-1 is determined by the stability of HIF-1α, which is determined largely by the activity of HIF-PHDs (40-42). Other factors could also influence the stability of HIF-1α. HIF1-PHDs also require α-KG as substrate to hydroxylate HIF-1α, resulting in the incorporation of a dioxygen into two substrates, HIF-1α and α-KG.

Enzymatically, the concentrations of oxygen and α-KG both affect the activity of HIF-PHDs. When oxygen levels are low, increasing α-KG has been shown to enhance the activity of HIF1-PHDs and decrease the stability of HIF-1α in BC cells. Previous studies have also demonstrated that modest variations in α-KG concentrations can significantly change HIF-PHDs activity (31,43,44). Moreover, α-KG is not only the substrate but also acts an allosteric activator of HIF1-PHDs by increasing its affinity for oxygen, thereby destabilizing HIF-1α at very low concentrations of oxygen (45,46). Previously, Dr. Xu's group identified a pathway to regulate α-KG levels by P4H in BC cells: the elevated expression of P4H in BC cells used α-KG to hydroxylate collagen, hence, depleting α-KG levels in BC cells, thereby stabilizing HIF-1α protein and promoting BC metastasis (10-12). We found that the increased α-KG levels decreased HIF-1α protein level, but did not significantly change collagen hydroxylation level in this study. As the substrate of 2-oxoglutarate-dependent dioxygenases, α-KG also affects the activity of P4H. But the affinity of HIF1-PHDs for α-KG is much higher than P4H (47).

α-KG is mainly produced from the flux of TCAC. In the flux of TCAC, malate could be dehydrogenated by malate dehydrogenase to produce NADH and oxaloacetate or catalyzed by ME2 to generate NAD(P)H and pyruvate through oxidative decarboxylation. ME2 competes with malate dehydrogenase for malate, therefore reducing the flux from malate to oxaloacetate and to TCAC. Thus, downregulating the expression of ME2 might cause a large

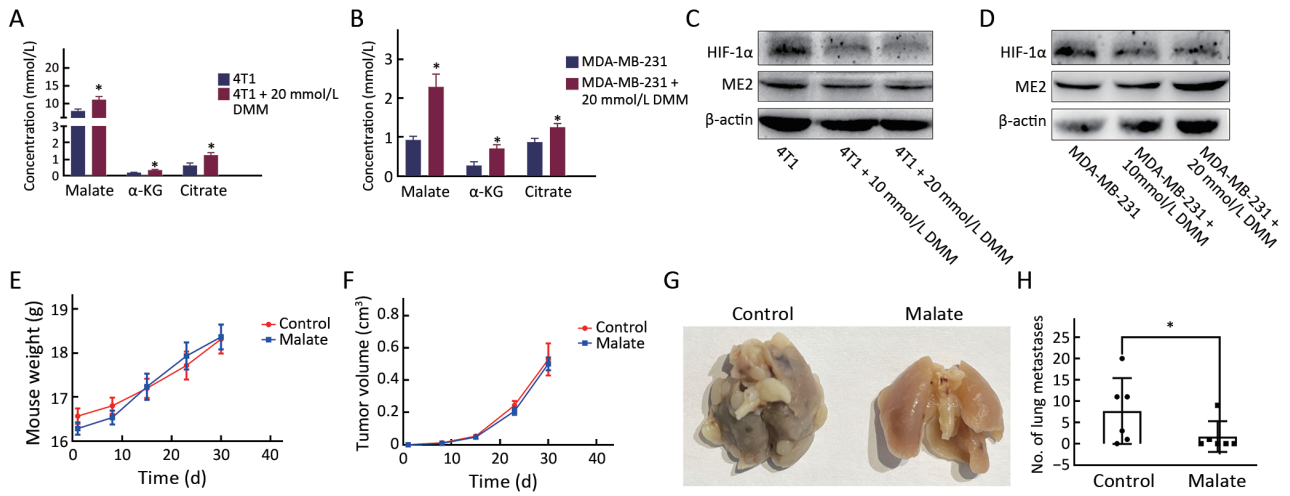

Figure 6 Effect of malate treatment on breast cancer cells. Cells were incubated in medium containing indicated concentrations of dimethyl malate (DMM) and cultured under 1% hypoxia for 4 h, and then analyzed. (A,B) Concentrations of malate, α-KG, and citrate in cells with or without DMM under hypoxia; (C,D) HIF-1α in 4T1 and MDA-MB-231 with or without DMM under hypoxia; (E,F) 4T1 cells were implanted orthotopically into mammary fat pads of BALB/c mice. Mice were randomly divided into two groups and injected intraperitoneally with PBS (control) or malate (50 mg/kg, dissolved in PBS) daily for three weeks. Body weight and tumor growth curve of BALB/c mice treatment with or without malate; (G,H) Lung metastatic nodules. *, P<0.05; **, P<0.01. α-KG, α-ketoglutarate; HIF-1α, hypoxia-inducible factor-1α; PBS, phosphate buffer saline; ME2, malic enzyme 2.

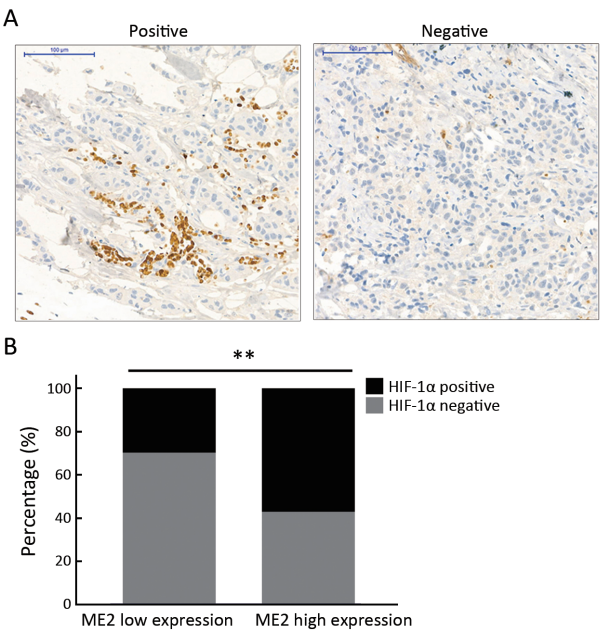

Figure 7 ME2 expression is associated with HIF-1α level in human BC. The 100 female BC patients were analyzed by IHC. (A) Representative IHC results of HIF-1α in human BC specimens. The scale bar is 100 μm; (B) Association between HIF-1α and ME2 expression (P=0.008). **, P<0.01. ME2, malic enzyme 2; HIF-1α, hypoxia-inducible factor-1α; BC, breast cancer; IHC, immunohistochemistry.

accumulation of malate in BC cells. Under hypoxia, as oxidative phosphorylation is inhibited (48-50) and NADH/NAD ratio increases (51,52), we hypothesized that the intermediates in the TCAC flux would undergo thermodynamic re-equilibration, which would lead to an increase in other TCAC intermediate levels, including α-KG. We showed that ME2 knockout or knockdown increased not only malate, but also α-KG and citrate levels in BC cells exposed to hypoxia. The increased levels of α-KG were associated with a decreased level of HIF-1α protein. Exogenous malate and α-KG exerted a similar effect on HIF-1α as ME2 knockdown or knockout. Thus, these results suggested that ME2 knockdown or knockout reduced HIF-1α protein levels by increasing α-KG levels in BC cells. Since HIF-1 signaling pathways are known to play important roles in BC metastasis (37,38,53), we proposed that metastasis inhibition induced by ME2 knockout or knockdown could be interpreted as follows: ME2 knockout induced accumulation of TCAC intermediates, including α-KG which destabilized HIF-1α by enhancing HIF1-PHDs activity, and eventually inhibited HIF-1α-mediated metastasis signaling.

The clinical evidence also suggests that ME2 expression is associated with BC metastasis. Patients with elevated

expression of ME2 had a worse survival than those with low expression of ME2. Elevated ME2 expression was related to lymph node metastasis, positive vascular cancer embolus, and pathological staging progression, all of which are key indicators of poor prognosis in BC patients. As metastasis accounts for 90% of BC-related deaths (5,6), and as elevated expression of ME2 is significantly correlated with survival rate (*Figure 1C*), we hypothesized a close link between ME2 expression and BC metastasis. Using 4T1 orthotopic BC *in vivo* model, we provided evidence that ME2 knockout nearly completely inhibited 4T1 cell lung metastasis.

Conclusions

We provide experimental and clinical evidence that ME2 plays a part in BC metastasis and interpret an underlying mechanism by which ME2 promotes BC metastasis. We demonstrate that ME2 promotes metastasis via regulating α-KG to stabilize HIF-1α in BC cells under hypoxia.

Acknowledgements

This study was supported in part by the China Natural Sciences Foundation projects (No. 81772947).

Footnote

Conflicts of Interest: The authors have no conflicts of interest to declare.

References

1. Sung H, Ferlay J, Siegel RL, et al. Global cancer statistics 2020: GLOBOCAN estimates of incidence and mortality worldwide for 36 cancers in 185 countries. CA Cancer J Clin 2021;71:209-49.
2. Sun D, Cao M, Li H, et al. Cancer burden and trends in China: a review and comparison with Japan and South Korea. Chin J Cancer Res 2020;32:129-39.
3. Chen W, Sun K, Zheng R, et al. Cancer incidence and mortality in China, 2014. Chin J Cancer Res 2018; 30:1-12.
4. DeSantis CE, Ma J, Gaudet MM, et al. Breast cancer statistics, 2019. CA Cancer J Clin 2019;69:438-51.
5. Gupta GP, Massagué J. Cancer metastasis: building a framework. Cell 2006;127:679-95.
6. Lambert AW, Pattabiraman DR, Weinberg RA. Emerging biological principles of metastasis. Cell 2017;168:670-91.
7. Gilkes DM, Semenza GL. Role of hypoxia-inducible factors in breast cancer metastasis. Future Oncol 2013;9:1623-36.
8. Semenza GL. Defining the role of hypoxia-inducible factor 1 in cancer biology and therapeutics. Oncogene 2010;29:625-34.
9. Wong CC, Gilkes DM, Zhang H, et al. Hypoxia-inducible factor 1 is a master regulator of breast cancer metastatic niche formation. Proc Natl Acad Sci U S A 2011;108:16369-74.
10. Xiong G, Stewart RL, Chen J, et al. Collagen prolyl 4-hydroxylase 1 is essential for HIF-1alpha stabilization and TNBC chemoresistance. Nat Commun 2018;9:4456.
11. Gilkes DM, Chaturvedi P, Bajpai S, et al. Collagen prolyl hydroxylases are essential for breast cancer metastasis. Cancer Res 2013;73:3285-96.
12. Xiong G, Deng L, Zhu J, et al. Prolyl-4-hydroxylase α subunit 2 promotes breast cancer progression and metastasis by regulating collagen deposition. BMC Cancer 2014;14:1.
13. Chang GG, Tong L. Structure and function of malic enzymes, a new class of oxidative decarboxylases. Biochemistry 2003;42:12721-33.
14. Loeber G, Infante AA, Maurer-Fogy I, et al. Human NAD+-dependent mitochondrial malic enzyme. cDNA cloning, primary structure, and expression in *Escherichia coli*. J Biol Chem 1991;266:3016-21.
15. Loeber G, Maurer-Fogy I, Schwendenwein R. Purification, cDNA cloning and heterologous expression of the human mitochondrial NADP$^+$-dependent malic enzyme. Biochem J 1994;304:687-92.
16. Jiang P, Du W, Mancuso A, et al. Reciprocal regulation of p53 and malic enzymes modulates metabolism and senescence. Nature 2013;493:689-93.
17. Ren JG, Seth P, Clish CB, et al. Knockdown of malic enzyme 2 suppresses lung tumor growth, induces differentiation and impacts PI3K/AKT signaling. Sci Rep 2014;4:5414.
18. Chang YL, Gao HW, Chiang CP, et al. Human mitochondrial NAD(P)$^+$-dependent malic enzyme participates in cutaneous melanoma progression and invasion. J Invest Dermatol 2015;135:807-15.
19. Cheng CP, Huang LC, Chang YL, et al. The

mechanisms of malic enzyme 2 in the tumorigenesis of human gliomas. Oncotarget 2016;7:41460-72.
20. Hsieh JY, Li SY, Tsai WC, et al. A small-molecule inhibitor suppresses the tumor-associated mitochondrial NADP+-dependent malic enzyme (ME2) and induces cellular senescence. Oncotarget 2015;6:20084-98.
21. Woo SH, Yang LP, Chuang HC, et al. Down-regulation of malic enzyme 1 and 2: Sensitizing head and neck squamous cell carcinoma cells to therapy-induced senescence. Head Neck 2016;38(1 suppl): E934-40.
22. Ran FA, Hsu PD, Wright J, et al. Genome engineering using the CRISPR-Cas9 system. Nat Protoc 2013;8:2281-308.
23. Passonneau JV, Lowry OH. Enzymatic analysis: a practical guide. Totowa: Humana Press, 1993.
24. Amin MB, Greene FL, Edge SB, et al. The Eighth Edition AJCC Cancer Staging Manual: Continuing to build a bridge from a population-based to a more "personalized" approach to cancer staging. CA Cancer J Clin 2017;67:93-9.
25. Frank GA, Danilova NV, Andreeva I, et al. WHO classification of tumors of the breast, 2012. Arkh Patol (in Russian) 2013;75:53-63.
26. Fitzgibbons PL, Dillon DA, Alsabeh R, et al. Template for reporting results of biomarker testing of specimens from patients with carcinoma of the breast. Arch Pathol Lab Med 2014;138:595-601.
27. Fedchenko N, Reifenrath J. Different approaches for interpretation and reporting of immunohistochemistry analysis results in the bone tissue — a review. Diagn Pathol 2014;9:221.
28. Potharaju M, Mathavan A, Mangaleswaran B, et al. Clinicopathological analysis of HIF-1α and TERT on survival outcome in glioblastoma patients: A prospective, single institution study. J Cancer 2019;10:2397-406.
29. Nalwoga H, Ahmed L, Arnes JB, et al. Strong expression of hypoxia-inducible factor-1α (HIF-1α) is associated with Axl expression and features of aggressive tumors in African breast cancer. PLoS One 2016;11:e0146823.
30. Ge J, Cui H, Xie N, et al. Glutaminolysis promotes collagen translation and stability via α-ketoglutarate-mediated mTOR activation and proline hydroxylation. Am J Respir Cell Mol Biol 2018;58:378-90.
31. Tennant DA, Frezza C, MacKenzie ED, et al. Reactivating HIF prolyl hydroxylases under hypoxia results in metabolic catastrophe and cell death. Oncogene 2009;28:4009-21.
32. Rankin EB, Giaccia AJ. Hypoxic control of metastasis. Science 2016;352:175-80.
33. Vaupel P, Höckel M, Mayer A. Detection and characterization of tumor hypoxia using pO2 histography. Antioxid Redox Signal 2007;9:1221-35.
34. Vaupel P, Mayer A, Briest S, et al. Oxygenation gain factor: a novel parameter characterizing the association between hemoglobin level and the oxygenation status of breast cancers. Cancer Res 2003;63:7634-7.
35. Lu X, Kang Y. Hypoxia and hypoxia-inducible factors: master regulators of metastasis. Clin Cancer Res 2010;16:5928-35.
36. Rankin EB, Nam JM, Giaccia AJ. Hypoxia: Signaling the metastatic cascade. Trends Cancer 2016;2: 295-304.
37. Semenza GL. Targeting HIF-1 for cancer therapy. Nat Rev Cancer 2003;3:721-32.
38. Unruh A, Ressel A, Mohamed HG, et al. The hypoxia-inducible factor-1α is a negative factor for tumor therapy. Oncogene 2003;22:3213-20.
39. Shenoy N, Dronca R, Quevedo F, et al. Low hypoxia inducible factor-1α (HIF-1α) expression in testicular germ cell tumors — a major reason for enhanced chemosensitivity? Chin J Cancer Res 2017;29:374-8.
40. Fong GH, Takeda K. Role and regulation of prolyl hydroxylase domain proteins. Cell Death Differ 2008;15:635-41.
41. Berra E, Benizri E, Ginouvès A, et al. HIF prolyl-hydroxylase 2 is the key oxygen sensor setting low steady-state levels of HIF-1α in normoxia. EMBO J 2003;22:4082-90.
42. Lee JW, Bae SH, Jeong JW, et al. Hypoxia-inducible factor (HIF-1) α: its protein stability and biological functions. Exp Mol Med 2004;36:1-12.
43. Koivunen P, Hirsilä M, Günzler V, et al. Catalytic properties of the asparaginyl hydroxylase (FIH) in the oxygen sensing pathway are distinct from those of its prolyl 4-hydroxylases. J Biol Chem 2004;279: 9899-904.
44. Loenarz C, Schofield CJ. Expanding chemical biology

of 2-oxoglutarate oxygenases. Nat Chem Biol 2008;4:152-6.
45. Iommarini L, Porcelli AM, Gasparre G, et al. Non-canonical mechanisms regulating hypoxia-inducible factor 1α in cancer. Front Oncol 2017;7:286.
46. MacKenzie ED, Selak MA, Tennant DA, et al. Cell-permeating alpha-ketoglutarate derivatives alleviate pseudohypoxia in succinate dehydrogenase-deficient cells. Mol Cell Biol 2007;27:3282-9.
47. Myllyharju J. Prolyl 4-hydroxylases, key enzymes in the synthesis of collagens and regulation of the response to hypoxia, and their roles as treatment targets. Ann Med 2008;40:402-17.
48. Wheaton WW, Chandel NS. Hypoxia. 2. Hypoxia regulates cellular metabolism. Am J Physiol Cell Physiol 2011;300:C385-93.
49. Fuhrmann DC, Brüne B. Mitochondrial composition and function under the control of hypoxia. Redox Biol 2017;12:208-15.
50. Solaini G, Baracca A, Lenaz G, et al. Hypoxia and mitochondrial oxidative metabolism. Biochim Biophys Acta 2010;1797:1171-7.
51. Alberti KG. The biochemical consequences of hypoxia. J Clin Pathol Suppl (R Coll Pathol) 1977; 3:14-20.
52. Garofalo O, Cox DW, Bachelard HS. Brain levels of NADH and NAD+ under hypoxic and hypoglycaemic conditions *in vitro*. J Neurochem 1988;51:172-6.
53. Muz B, de la Puente P, Azab F, et al. The role of hypoxia in cancer progression, angiogenesis, metastasis, and resistance to therapy. Hypoxia (Auckl) 2015;3:83-92.

Cite this article as: You D, Du D, Zhao X, Li X, Ying M, Hu X. Mitochondrial malic enzyme 2 promotes breast cancer metastasis via stabilizing HIF-1α under hypoxia. Chin J Cancer Res 2021;33(3):308-322. doi: 10.21147/j.issn.1000-9604.2021.03.03

Table S1 Univariate and multivariate analysis of survival rate on ME2 expression and clinicopathological indicators

Variables	No. of patients examined	Univariate analysis		Multivariate analysis		
		χ^2	P	HR	95% CI	P
Age (year)		0.019	0.890			
<50	60					
≥50	40					
T staging		2.238	0.135			
Tis+T1	34					
T2+T3	66					
Lymph node metastasis		10.989	0.001	3.878	1.38–10.87	0.010
No	58					
Yes	42					
Pathological staging		12.711	0.000			
0+I+IIA	60					
IIB+III	40					
Vascular cancer embolus		1.268	0.260			
No	83					
Yes	17					
ME2 expression		5.527	0.019			
Low	37					
High	63					

ME2, malic enzyme 2; HR, hazard ratio; 95% CI, 95% confidence interval.

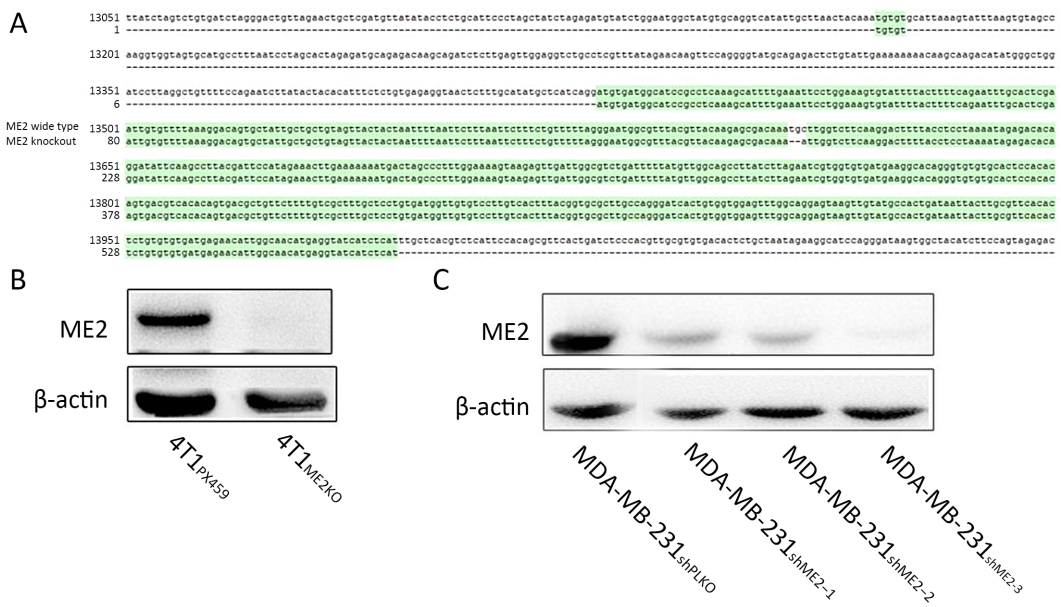

Figure S1 Characterization of 4T1 ME2 knockout and MDA-MB-231 ME2 knockdown. (A) DNA sequence identification of targeted genomic region in 4T1 ME2 wild-type and 4T1 ME2 knockout cells; (B) 4T1 ME2 knockout effect was checked by western blot; (C) MDA-MB-231 ME2 knockdown effect was checked by western blot. ME2, malic enzyme 2.